

Higgs self-coupling measurements at the LHC

Matthew J. Dolan,¹ Christoph Englert,¹ and Michael Spannowsky¹

¹*Institute for Particle Physics Phenomenology, Department of Physics,
Durham University, DH1 3LE, United Kingdom*

Both the ATLAS and CMS collaborations have reported a Standard Model Higgs-like excess at around $m_h = 125$ GeV. If an SM-like Higgs particle is discovered in this particular mass range, an important additional test of the SM electroweak symmetry breaking sector is the measurement of the Higgs self-interactions. We investigate the prospects of measuring the Higgs self-coupling for $m_h = 125$ GeV in the dominant SM decay channels in boosted and unboosted kinematical regimes. We further enhance sensitivity by considering diHiggs systems recoiling against a hard jet. This configuration exhibits a large sensitivity to the Higgs self-coupling which can be accessed in subjet-based analyses. Combining our analyses allows constraints to be set on the Higgs self-coupling at the LHC.

I. INTRODUCTION

The Standard Model (SM) Higgs [1] has recently been excluded at the 95% confidence level from 129 (127.5) GeV to 539 (600) GeV by measurements performed by ATLAS (CMS) [2]. In addition, the Higgs mass bound from LEP2 was raised from 114.4 GeV [3] to 117.5 GeV by ATLAS. Both ATLAS and CMS have also observed tantalizing hints for a SM-like Higgs at a mass $m_h \simeq 125$ GeV with local significances of 2.5σ and 2.8σ , respectively. In the same mass region, the $D\phi$ and CDF collaborations observe an excess with a local significance of 2.2σ for the combination of their data sets [4].

Breaking down these results into the individual search channels has triggered some effort to pin down the properties of the observed excess in the SM and beyond [5]. These analyses are the first steps of a spectroscopy program which targets the properties of a newly discovered particle if the excess at 125 GeV becomes statistically significant. Strategies to determine spin- and \mathcal{CP} quantum numbers, and the couplings to fermions and gauge bosons of a 125 GeV resonance with SM-like cross sections have been discussed in the literature [6, 7]. A determination of the Higgs self-interaction, however, which is crucial for a measurement of the symmetry breaking sector remains challenging in the context of the SM (this can change in BSM scenarios [8]). Even for scenarios where the Higgs is close to the $h \rightarrow W^+W^-$ threshold, statistics at the LHC in $pp \rightarrow hh + X$ is extremely limited [9–11], so that formulating constraints on the Higgs self-coupling requires end-of-LHC-lifetime statistics if possible at all*.

The Higgs self-coupling in the SM follows from equating out the Higgs potential after the Higgs doublet is expanded around the electroweak symmetry breaking vacuum expectation value, $H = (0, v + h)^T/\sqrt{2}$ in unitary

gauge:

$$V(H^\dagger H) = \mu^2 H^\dagger H + \eta (H^\dagger H)^2 \\ \supset \frac{1}{2} m_h^2 h^2 + \sqrt{\frac{\eta}{2}} m_h h^3 + \frac{\eta}{4} h^4, \quad (1)$$

where $m_h^2 = \eta v^2/2$, and $v^2 = -\mu^2/\eta$. Since symmetry breaking in the SM relies on $\mu^2 < 0$ and $\eta > 0$, the partial experimental reconstruction of the Higgs potential via the measurement of the trilinear Higgs vertex and its comparison to SM quantities (*e.g.* $2\eta = g^2 m_h^2/m_W^2$) is necessary to verify symmetry breaking due to a SM-like Higgs sector. Strictly speaking, a similar program needs to be carried out for the quartic Higgs vertex to fully reconstruct the Higgs potential by measurements. This task is, however, even more challenging due to an even smaller cross section of triple Higgs production [13].

A process at hadron colliders which is sensitive to the trilinear Higgs coupling is the previously mentioned Higgs pair production $pp \rightarrow hh + X$ via gluon fusion. Consequently, this process has already been studied in the literature in detail [14–16]. From the known results it is clear that the LHC's potential towards measuring the trilinear coupling only in this single channel is insufficient. Combining different Higgs decay final states improves this situation, but exhausting the entire LHC search potential requires also discussing the machine's capability to constrain the trilinear Higgs coupling in different kinematical regimes.

Different properties of signal and background processes in *e.g.* boosted final states as compared to unboosted kinematics allows us to access Higgs decay channels which are impossible to isolate from the background in a more inclusive search. This has impressively been demonstrated in the context of subjet-based analysis techniques [17], which have proven successful during the 7 TeV LHC run [19]. In addition to that, initial state radiation can be an important effect when considering energetic final states. A diHiggs system recoiling against a hard hadronic jet accesses an entirely new kinemat-

*A related analysis of Higgs physics at a future linear collider can be found in Ref. [12].

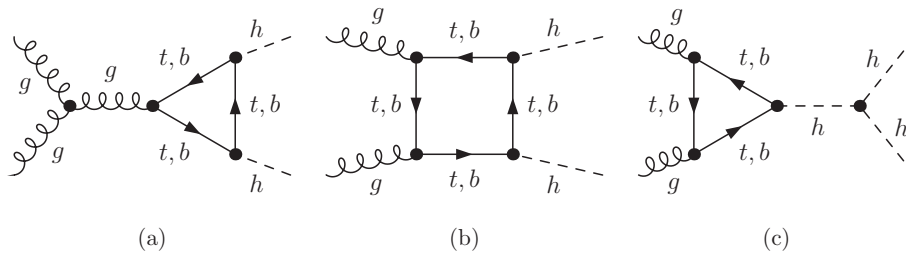


FIG. 1: Sample Feynman graphs contributing to $pp \rightarrow hh + X$.

cal configuration[†], which is characterized by a large di-higgs invariant mass, but with a potentially smaller Higgs s -channel suppression than encountered in the back-to-back configuration of $gg \rightarrow hh$.

The goal of this paper is to provide a comparative study of the prospects of the measurement of the trilinear Higgs coupling applying contemporary simulation and analysis techniques. In the light of recent LHC measurements, we focus our eventual analyses on $m_h = 125$ GeV. However, we also put this particular mass into the context of a complete discussion of the sensitivity towards the trilinear Higgs coupling over the entire Higgs mass range $m_h \lesssim 1$ TeV. As we will see, $m_h \simeq 125$ GeV is a rather special case. Since Higgs self-coupling measurements involve end-of-lifetime luminosities we base our analyses on a center-of-mass energy of 14 TeV.

We begin with a discussion of some general aspects of double Higgs production, before we review inclusive searches for $m_h = 125$ GeV in the $pp \rightarrow hh + X$ channel in Sec. II C. We discuss boosted Higgs final states in $pp \rightarrow hh + X$ in Sec. III B 2 before we discuss $pp \rightarrow hh + j + X$ with the Higgses recoiling against a hard jet in Sec. III. Doing so we investigate the potential sensitivity at the parton- and signal-level to define an analysis strategy before we apply it to the fully showered and hadronized final state. We give our conclusions in Sec. IV.

II. HIGGS PAIR PRODUCTION AT THE LHC

A. General Remarks

Inclusive Higgs pair production has already been studied in Refs. [14–16] so we limit ourselves to the details that are relevant for our analysis.

Higgs pairs are produced at hadron colliders such as the LHC via a range of partonic subprocesses, the most dominant of which are depicted in Fig. 1. An approximation which is often employed in phenomenological studies is the heavy top quark limit, which gives rise to effective

ggh and $gghh$ interactions [20]

$$\mathcal{L}_{\text{eff}} = \frac{1}{4} \frac{\alpha_s}{3\pi} G_{\mu\nu}^a G^{a\mu\nu} \log(1 + h/v), \quad (2)$$

which upon expansion leads to

$$\mathcal{L} \supset + \frac{1}{4} \frac{\alpha_s}{3\pi v} G_{\mu\nu}^a G^{a\mu\nu} h - \frac{1}{4} \frac{\alpha_s}{6\pi v^2} G_{\mu\nu}^a G^{a\mu\nu} h^2. \quad (3)$$

Studying these operators in the $hh + X$ final state should in principle allow the Higgs self-coupling to be constrained via the relative contribution of trilinear and quartic interactions to the integrated cross section. Note that the operators in Eq. (3) have different signs which indicates important interference between the (nested) three- and four point contributions to $pp \rightarrow hh + X$ already at the effective theory level.

On the other hand, it is known that the effective theory of Eq. (3) insufficiently reproduces all kinematical properties of the full theory if the interactions are probed at momentum transfers $Q^2 \gtrsim m_t^2$ [11] and the massive quark loops are resolved. Since our analysis partly relies on boosted final states, we need to take into account the full one-loop contribution to di-higgs production to realistically model the phenomenology.

B. Parton-level considerations

In order to properly take into account the full dynamics of Higgs pair production in the SM we have implemented the matrix element that follows from Fig. 1 in the VBFNLO framework [21] with the help of the FEYNARTS/FORMCALC/LOOPTOOLS packages [22], with modifications such to include a non-SM trilinear Higgs coupling[‡]. Our setup allows us to obtain event files according to the Les Houches standard [23], which can be straightforwardly interfaced to parton showers. Decay correlations are trivially incorporated due to the spin-0 nature of the SM Higgs boson.

[†]The phenomenology of such configurations can also be treated separately from radiative correction contributions to $pp \rightarrow hh + X$.

[‡]The signal Monte Carlo code underlying this study is planned to become part of the next update of VBFNLO and is available upon request until then.

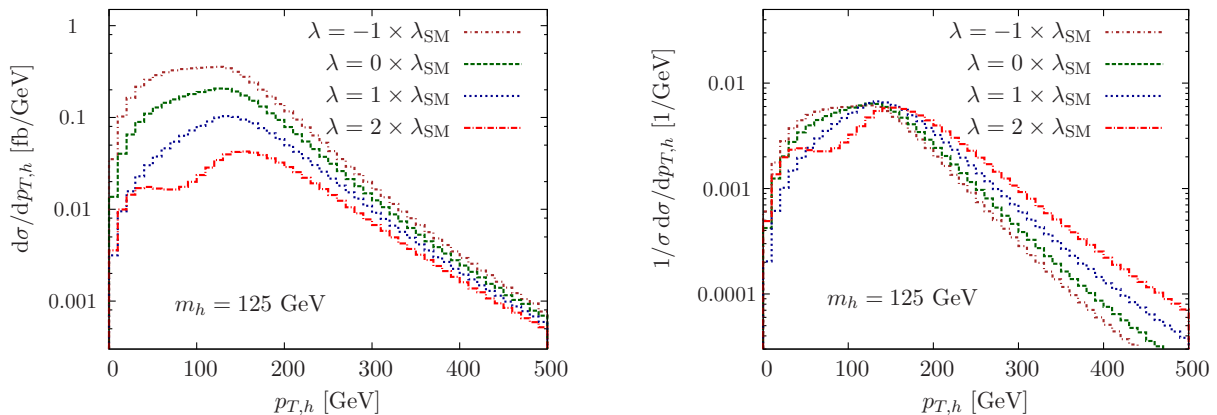


FIG. 2: Comparison of the (normalized) $p_{T,h}$ distributions in $pp \rightarrow hh + X$ for different multiples of the trilinear Higgs coupling λ ($m_t = 172.5$ GeV and $m_b = 4.5$ GeV using CTEQ611 parton densities).

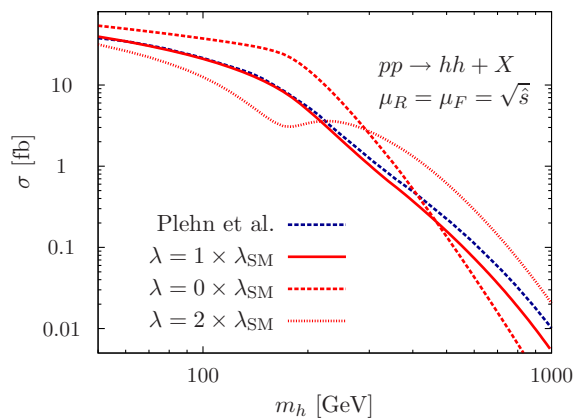


FIG. 3: Comparison of $pp \rightarrow hh + X$. We choose $m_t = 175$ GeV as in Ref. [14], from which we also obtain the dashed blue reference line, and $m_b = 4.5$ GeV and we use the CTEQ611 parton distributions.

The resulting inclusive hadronic cross sections are plotted in Fig. 3, where we also show results for non-SM trilinear couplings, varied around the SM value (see Eq. (1))

$$\lambda_{\text{SM}} = \sqrt{\frac{\eta}{2}} m_h. \quad (4)$$

Note that choosing a value different from λ_{SM} does not yield a meaningful potential in terms of Eq. (1), but allows to constrain λ in hypothesis tests using, *e.g.*, the CL_s method [24].

We also show the result of Ref. [14] for comparison and find excellent agreement in total, keeping in mind that the results of Ref. [14] were obtained using the GRV parametrizations of parton luminosities [25], which are different from the CTEQ611 [26] set that we employ for the remainder of this paper[§].

Interference between the different contributions depicted in Fig. 3 becomes obvious for the differently chosen Higgs self-couplings. We also learn from Fig. 3 that the dihiggs cross section has a fairly large dependence on the particular value of the trilinear coupling for a $m_h = 125$ GeV Higgs boson. The qualitative Higgs mass dependence for different values of the trilinear self-coupling in Fig. 3 is easy to understand: The Higgs propagator in Fig. 1 (c) is always probed off-shell at fairly large invariant masses; this renders the triangle contributions subdominant compared to the box contributions of Fig. 1 (b). For Higgs masses close to the mass of the loop-dominating top quark, we have $s \simeq 4m_t^2$, which results in resonant contributions of the three-point functions of Fig. 1 (c), well-known from one-loop $gg \rightarrow h$ production [27]. This ameliorates the s -channel suppression of the trilinear coupling-sensitive triangle graphs and causes the dependence of the cross section on the trilinear coupling to become large at around $m_h \lesssim m_t$.

To gain sensitivity beyond total event counts, it is important to isolate the region of phase space which is most sensitive to modifications of the trilinear coupling in order to set up an analysis strategy which targets the trilinear self-coupling most effectively. At the parton level, there is only a single phenomenologically relevant observable to hh production, which can be chosen as the Higgs transverse momentum $p_{T,h}$. In Fig. 2 we show the differential $p_{T,h}$ distribution for different values of λ and $m_h = 125$ GeV. The dip structure for $\lambda > \lambda_{\text{SM}}$ results again from phase space regions characterized by $s \sim 4m_t^2$, which are available if $m_h < m_t$, and the resulting maximally destructive interference with the box contributions.

The above points suffice to give a qualitative assessment of the prospects of measurements of λ in the $pp \rightarrow hh + X$ channel:

- the Higgs bosons from inclusive dihiggs productions

[§]Using the integration-mode of FORMCALC/LOOPTOOLS with the

CTEQ611 set we obtain perfect agreement.

	$\xi = 0$	$\xi = 1$	$\xi = 2$	$b\bar{b}WW$	ratio to $\xi = 1$
cross section before cuts	59.48	28.34	13.36	877500	$3.2 \cdot 10^{-5}$
1 isolated lepton	7.96	3.76	1.74	254897	$1.5 \cdot 10^{-5}$
MET + jet cuts	1.54	0.85	0.44	66595.7	$1.2 \cdot 10^{-5}$
hadronic W reconstruction	0.59	0.33	0.17	38153.3	$0.9 \cdot 10^{-5}$
kinematic Higgs reconstruction	0.028	0.017	0.007	205.1	$8.3 \cdot 10^{-5}$

TABLE I: Signal and background cross sections in fb for $hh \rightarrow b\bar{b}W^+W^-$. The Higgs self-coupling is scaled in multiples of the Standard Model value $\lambda = \xi \times \lambda_{\text{SM}}$, Eq. (4). The background is $b\bar{b}W^+W^-$ production discussed at NLO in Ref. [28] ($K \simeq 1.5$).

are naturally boosted $p_{T,h} \gtrsim 100$ GeV,

- interference leads to an *a priori* λ -sensitive phenomenology for $m_h \simeq 125$ GeV,
- identical interference effects also cause the bulk of the sensitivity to λ to follow from configurations with $p_{T,h} \sim 100$ GeV, while the $p_{T,h}$ shape at large values becomes similar for different values of λ due to decoupling the triangle contributions at large partonic $\sqrt{\hat{s}}$,
- the cross section shows a dependence on the trilinear coupling of $\Delta\sigma/\sigma_{\text{SM}} \simeq 50\%$ when varying $\lambda \in [0, 2\lambda_{\text{SM}}]$.

We conclude our parton-level discussion of dihiggs production by noting that the higher-order corrections [15], which result in a total K factor of $\sigma^{\text{NLO}}/\sigma^{\text{LO}} \simeq 1.85$, result from a large contribution from real parton emission. This is a characteristic trait of processes involving color-singlet final states at leading order, for which plenty of phase space for extra parton emission in addition to new initial-state parton combinatorics becomes available at next-to-leading order (NLO). Similar observations have been made for $pp \rightarrow VV + X$, where $V = W^\pm, Z, \gamma$ [29]. The discussed characteristics of $pp \rightarrow hh + X$ are therefore not distorted when including NLO precision, and the parton shower will capture the characteristic features of the cross section upon normalizing to the NLO inclusive rate.

C. Inclusive Higgs Pair Searches

To measure λ for a 125 GeV Higgs we need to isolate modifications of $pp \rightarrow hh + X$ cross sections around $\sigma^{\text{NLO}}(hh + X) = 28.4$ fb from the Higgses' exclusive decay channels. Given the small total inclusive cross section[¶], it is clear that even for $\sqrt{s} = 14$ TeV and a target luminosity of $\mathcal{O}(1000\text{fb}^{-1})$ we need to focus on the Higgs decay channels with the largest branching ratios to phenomenologically visible final states to observe $pp \rightarrow$

$hh + X$. These are [31] $h \rightarrow b\bar{b}$ (59.48%), $h \rightarrow W^+W^-$ (20.78%), and $h \rightarrow \tau\tau$ (6.12%). The decay $h \rightarrow ZZ$ (2.55%) is limited by the decays of the Z bosons to the clean leptonic final states $Z \rightarrow e^+e^-, \mu^+\mu^-$ (6.67%) (yielding $\text{BR}(h \rightarrow e^+e^- + \mu^+\mu^-) = 0.013\%$). Hadronic Z decay modes can only be accessed in the boosted regime, which is not feasible for $m_h = 125$ GeV [32].

We do not consider the final state $hh \rightarrow b\bar{b}\gamma\gamma$. A feasibility study for this particular channel was already presented in Ref. [9]. A realistic assessment of the sensitivity in $b\bar{b}\gamma\gamma$ depends on a realistic simulation of the diphoton fake rate due to multijet production, which is the dominant background to such an analysis, similar to Higgs searches in $h \rightarrow \gamma\gamma$. Details of the photon identification rely on the detector properties and the event selection approach, and we cannot address these issues in a realistic fashion. We focus in on $h \rightarrow b\bar{b}, W^+W^-, \tau^+\tau^-$ in the following.

We generate all (fully showered and hadronized) background samples with SHERPA [33] or MADEVENT [34]. The signal events are interfaced to HERWIG++ [35] for showering and hadronization.

1. $hh \rightarrow b\bar{b}b\bar{b}$

The exclusive decay to two $b\bar{b}$ pairs is the most obvious channel to check for sensitivity due to its large branching ratio for $m_h = 125$ GeV. Using b -tagging, it is also possible to access the intermediate invariant Higgs masses, for which the modifications due to $\lambda \neq \lambda_{\text{SM}}$ are well-pronounced.

Passing the trigger-level cuts is not a problem for the signal events: the Higgses are naturally boosted and the p_T -ordered b jets typically pass the staggered cuts on the transverse momentum $p_{T,j_1} > 100$ GeV, $p_{T,j_2} > 80$ GeV, $p_{T,j_3} > 50$ GeV, $p_{T,j_4} > 40$ GeV. However, as already mentioned, there is only one relevant scale to dihiggs production, and therefore our options to compete with the gigantic QCD $pp \rightarrow b\bar{b}b\bar{b} + X$ background are highly limited. Note that both Higgs bosons need to be reconstructed in order to be sensitive to the modifications of the trilinear coupling.

In total, inclusive dihiggs production with decay to four b quarks has a signal-over-background ratio S/B which is too bad to be a suitable search channel, already when we focus only on the QCD-induced four b

[¶]The total inclusive single Higgs production cross section is 16.5 pb [30] for comparison.

	$\xi = 0$	$\xi = 1$	$\xi = 2$	$b\bar{b}b\bar{b}$ [QCD]	$b\bar{b}b\bar{b}$ [ELW]	$b\bar{b}b\bar{b}$ [QCD/ELW]	ratio to $\xi = 1$
cross section before cuts	59.48	28.42	13.36	21165	16.5	160.35	$1.3 \cdot 10^{-3}$
trigger+no leptons	17.93	10.21	5.31	5581.2	8.0	38.85	$1.8 \cdot 10^{-3}$
fatjet cuts	13.73	8.23	4.50	4761.0	7.50	31.65	$1.7 \cdot 10^{-3}$
first Higgs rec + $2b$	1.55	1.02	0.60	235.22	0.75	1.32	$4.2 \cdot 10^{-3}$
second Higgs rec + $2b$	0.137	0.094	0.059	9.72	0.011	0.050	$9.6 \cdot 10^{-3}$

TABLE II: Signal and background cross sections in fb for $hh \rightarrow b\bar{b}b\bar{b}$ for boosted kinematics. The Higgs self-coupling is scaled in multiples of the Standard Model value $\lambda = \xi \times \lambda_{\text{SM}}$, Eq. (4). Signal and background are normalized to the respective NLO cross sections. NLO $b\bar{b}b\bar{b}$ production has been provided in Ref. [36] (inclusive $K \simeq 1.5$). The mixed QCD+electroweak production and the purely electroweak production is currently not known at NLO QCD precision, and we therefore use an identical correction factor as for the QCD-induced production.

background. Hence, this channel is not promising at the inclusive level and we revise it for boosted kinematics in Sec. III B 2.

2. $hh \rightarrow b\bar{b}W^+W^-$

To gain multiple phenomenological handles to deal with the contributing backgrounds while preserving a signal rate as large as possible we focus on $h \rightarrow b\bar{b}$ and $h \rightarrow (W \rightarrow jj)(W \rightarrow \nu l)$. The contributing background processes are $t\bar{t}$ and $b\bar{b}W^+W^-$ production and we can employ cuts on missing transverse energy (MET), lepton identification and p_T , and the reconstructed W resonance to reduce them.

We require exactly one isolated lepton with $p_{T,l} > 10$ GeV in the central part of the detector $|y| < 2.5$, where isolation means an hadronic energy deposit of $E_{T,\text{had}} < 0.1 E_{T,l}$ within a cone of $R = 0.3$ around the identified light-flavor lepton. In the next step we reconstruct the missing transverse energy (MET) \cancel{E}_T from all visible final state objects within the rapidity coverage $|y| < 4.5$ and require $\cancel{E}_T > 20$ GeV. Then, we use the anti-kT [45] algorithm as implemented in FASTJET [39] (which we use throughout this paper) to reconstruct jets with $R = 0.6$ and $p_T > 40$ GeV, and require at least four jets in $|y| < 4.5$. Afterwards we reconstruct the W boson by looping over all jet pairs. The jet pair that reconstructs the W mass best within $60 \text{ GeV} \leq m_{jj} \leq 100 \text{ GeV}$ is identified as the W boson, and we subsequently remove these jets from the event. Analogous to the W reconstruction we reconstruct the Higgs within $110 \text{ GeV} \leq m_{jj} \leq 140 \text{ GeV}$. To reduce the backgrounds and identify the signal contributions we use a double b -tag for the two jets which reconstruct the Higgs best. We use an efficiency of 60% with a fake rate of 2% in $|y| < 2.5$ [40]. Thus, if one of the Higgs jets is outside $|y| = 2.5$ our reconstruction fails.

The results of this analysis flow can be found in Tab. I. While the cuts bring down the background by a factor of 4×10^3 , they also reduce the signal by nearly the same amount (1.5×10^3). The requirement of two reconstructed Higgses has a strong effect on the background, however the initial cross-section (although inclusively generated)

is simply too large for these cuts to bring down the S/B for this channel to a level for it to be useful in constraining the Higgs trilinear coupling.

D. Boosted Higgs Pair Searches

Moving on to the discussion of boosted final states, we can potentially gain sensitivity in the dominant Higgs decay modes, *i.e.* in the $b\bar{b}$ channels [17]. The downside, however, is that we lose sensitivity to modifications of the trilinear couplings for harder Higgs bosons along the lines of Sec. II B. Nonetheless, a measurement of the magnitude of the diHiggs cross section is already an important task in itself.

Recently, in the so-called BDRS analysis [17], it has been shown that applying jet substructure techniques on fatjets is a powerful tool to discriminate boosted electroweak-scale resonances from large QCD backgrounds. The BDRS approach proposes to recombine jets using the Cambridge-Aachen (C/A) algorithm [43, 44] with a large cone size to capture all decay products of the boosted resonance. Then one works backward through the jet clustering and stops when the clustering meets a so-called "mass-drop" condition: $m_{j_1} < \mu m_j$ with $\mu = 0.66$ and $\min(p_{T,j_1}^2, p_{T,j_2}^2)/m_j^2 \Delta R_{j_1,j_2}^2 > y_{\text{cut}}$ using $y_{\text{cut}} = 0.09$. If this condition is not met the softer subjet j_2 is removed and the subjets of j_1 are tested for a mass drop. As soon as this condition is met browsing backward through the cluster history the algorithm stops. In a step called "filtering" the constituents of the two subjets which meet the mass drop condition are recombined using the (C/A) algorithm with $R_{\text{filt}} = \min(0.3, R_{b\bar{b}}/2)$. Only the three hardest filtered subjets are kept to reconstruct the Higgs boson and the two hardest filtered subjets are b -tagged. The filtering step reduces the active area of the jet tremendously and makes the Higgs-mass reconstruction largely insensitive to underlying event and pileup.

For the reconstruction of the boosted Higgs bosons in Sec. II D 1 and Sec. II D 2 we adopt this approach without modifications. It is worth noting that other techniques, possibly in combination with the BDRS approach, can improve on the Higgs reconstruction efficiency and can

	$\xi = 0$	$\xi = 1$	$\xi = 2$	$b\bar{b}\tau\tau$	$b\bar{b}\tau\tau$ [ELW]	bbww	ratio to $\xi = 1$
cross section before cuts	59.48	28.34	13.36	43.60	6.64	873000	$3.2 \cdot 10^{-5}$
reconstructed Higgs from τ s	4.05	1.94	0.91	1.4	0.52	1507.99	$1.9 \cdot 10^{-3}$
fatjet cuts	2.27	1.09	0.65	1.13	0.51	223.21	$4.8 \cdot 10^{-3}$
kinematic Higgs reconstruction ($m_{b\bar{b}}$)	0.41	0.26	0.15	0.083	0.034	9.50	$2.3 \cdot 10^{-2}$
Higgs with double b -tag	0.148	0.095	0.053	0.028	0.014	0.15	0.49

TABLE III: Signal and background cross sections in fb for $hh \rightarrow b\bar{b}\tau^+\tau^-$ for boosted kinematics. The Higgs self-coupling is scaled in multiples of the Standard Model value $\lambda = \xi \times \lambda_{\text{SM}}$, Eq. (4). The background comprises $t\bar{t}$ with decays to $t \rightarrow b\tau\nu_\tau$, and $b\bar{b}\tau^+\tau^-$ for pure electroweak and mixed QCD-electroweak production, normalized to the respective NLO rates. The $b\bar{b}W^+W^-$ NLO cross sections are provided in [28] ($K \simeq 1.5$), for the mixed and the purely electroweak contributions we infer the corrections from $Zb\bar{b}$ ($K \simeq 1.4$) and ZZ ($K \simeq 1.6$) production using MCFM [37, 38].

therefore increase the sensitivity of the following searches [18].

1. $hh \rightarrow b\bar{b}b\bar{b}$

As already pointed out, the Higgs bosons are naturally boosted, and requiring two fatjets subject to BDRS tagging [17] can improve the very bad S/B in the conventional $pp \rightarrow b\bar{b}b\bar{b} + X$ search without losing too much of the diHiggs signal cross section.

In the analysis, we veto events with light leptons $p_{T,l} > 10$ GeV in $|y| < 2.5$ to reduce $t\bar{t}$, where the leptons are again assumed isolated if $E_{T,\text{had}} < 0.1E_{T,l}$ within $R < 0.3$. We need to make sure that the events we want to isolate pass the trigger level. For this reason, we recombine final state hadrons to jets with $R = 0.4$ and $p_T > 40$ GeV and require at least four jets and the following staggered cuts: $p_{T,j_1} > 100$ GeV, $p_{T,j_2} > 70$ GeV, $p_{T,j_3} > 50$ GeV. All jets have to be within detector coverage $|y| < 4.5$.

For the events that pass the trigger cuts, we apply a ‘‘fatjet’’ analysis, *i.e.* require at least two jets with $p_{T,j} > 150$ GeV and $R = 1.5$ in the event. We apply the BDRS approach to both of these fatjets using $\mu_{\text{cut}} = 0.66$ and $y_{\text{cut}} = 0.09$. The reconstructed Higgs jets need to reproduce the Higgs mass within a 20 GeV window: $115 \text{ GeV} \leq m_h \leq 135 \text{ GeV}$, and we additionally require that the two hardest filtered subjects are b -tagged.

The results are collected in Tab. II. Again, while the cuts allow an improvement in S/B by an nearly an order of magnitude, we are still left with a small signal rate on top of a very large background so that this channel is in the end also not promising.

2. $hh \rightarrow b\bar{b}\tau^+\tau^-$

A promising channel is diHiggs production with one Higgs decaying to a pair of τ leptons. This decay channel in association with two jets is one of the main search channels for single light Higgs production [46, 47] and has recently been used to put bounds on Higgs production by CMS [48]. The reconstruction of τ leptons is delicate

from an experimental point of view, and current analysis strategies mostly rely on semi-hadronic τ pair decays in the context of Higgs searches (see *e.g.* Ref. [48]). The τ identification is performed using likelihood methods [49] which do not allow a straightforward interpretation in terms of rectangular cuts used in *e.g.* Ref. [47]. Consequently, with likelihood τ taggers unavailable to the public, a reliable and realistic estimate is hard to obtain. For this reason, we choose a τ reconstruction efficiency of 80% with a negligible fake rate. This is not too optimistic in the light of the likelihood approaches of Ref. [49], bearing in mind that our analyses are based on end-of-lifetime luminosities, for which we may expect a significant improved τ reconstruction when data is better understood. We choose a large enough Higgs mass window for the reconstruction, in order to avoid a too large systematic pollution due to our assumption (in Ref. [48] CMS quotes a $\mathcal{O}(20\%)$ of the reconstructed Higgs mass).

In more detail, we require two τ jets, reproducing the Higgs mass within 50 GeV, $m_{\tau\tau} = m_h \pm 25$ GeV. Then we use the C/A algorithm to reconstruct fatjets with $R = 1.5$ and $p_{T,j} > 150$ GeV and require at least one fatjet in the event. Thereby we demand the fatjets to be sufficiently isolated from the τ s. We subsequently apply the BDRS approach to the fatjet with $\mu_{\text{cut}} = 0.66$ and $y_{\text{cut}} = 0.09$. The two hardest filtered subjects need to pass b tags and the reconstructed Higgs jet has to be in $m_h \pm 10$ GeV. B -tagging is performed for $|y| < 2.5$ and we assume an efficiency of 70% and a fake rate of 1% following Ref. [50].

The results are shown in Tab. III. The initial background cross-section looks very large due to it being inclusively generated. However, once we take into account the small branching ratio of $W \rightarrow \tau\nu$ this drops dramatically. After requiring two b -tagged jets which reconstruct the Higgs mass we are left with an S/B of nearly half for the $\xi = 1$ case (and nearly one in for $\xi = 0$). The cross-section is also reasonable, corresponding to 95 events for 1000 inverse femtobarns of luminosity. This channel is hence very promising indeed.

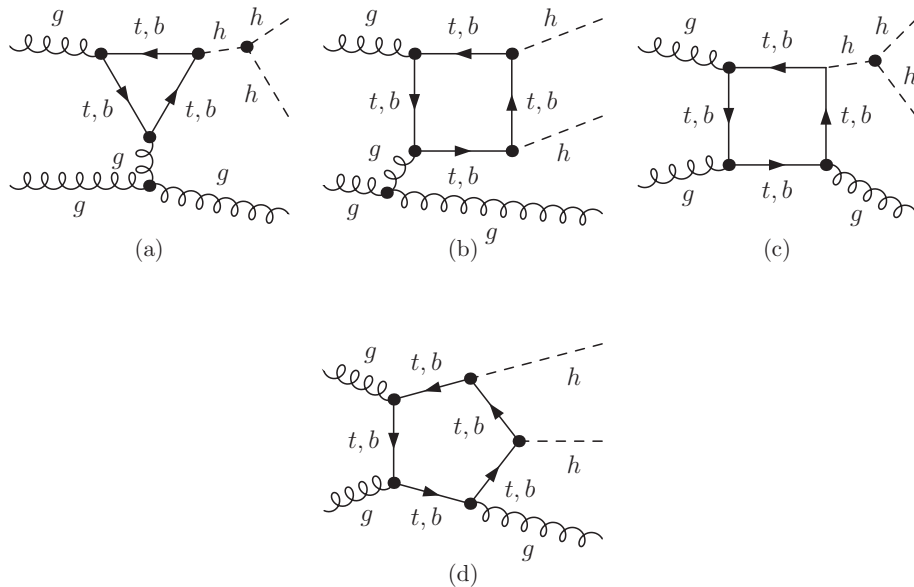


FIG. 4: Sample Feynman graphs contributing to $pp \rightarrow hh + j + X$. Not shown are the $qg, \bar{q}g$ and $q\bar{q}$ subprocesses.

III. HIGGS PAIR PRODUCTION IN ASSOCIATION WITH A HARD HADRONIC JET

A. Parton-Level considerations

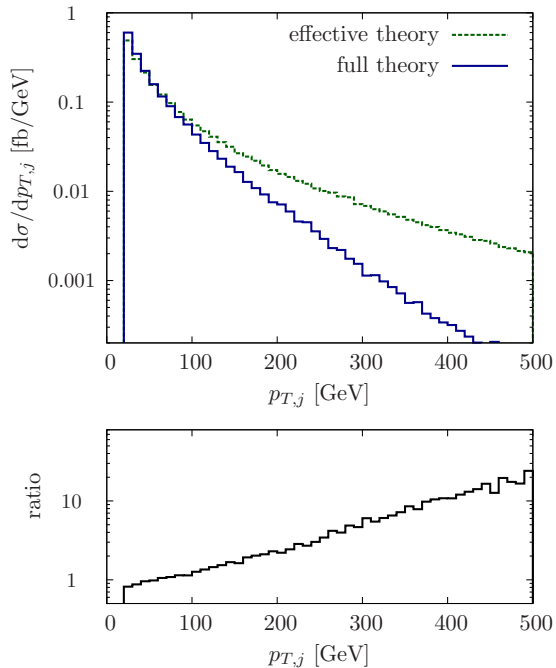


FIG. 5: Comparison of the $p_{T,j}$ spectrum for $pp \rightarrow hh + j + X$ production. Shown are distributions for the effective interaction (obtained with MADGRAPH v5 [34] via FEYNRULES [41] and UFO [42]), and the full one-loop matrix element calculation. We again choose $m_t = 172.5$ GeV and $m_b = 4.5$ GeV using CTEQ61l parton densities and $\mu_F = \mu_R = p_{T,j} + 2m_h$.

The qualitatively poor agreement of the effective theory of Eq. (3) with the full theory persists if additional jet radiation is included. Naively we could have expected that accessing smaller invariant masses in the Higgs system due to significant initial state radiation might result in a better agreement with the effective theory of Eq. (3). However, especially for hard jet emission, which allows the Higgs pairs to access large invariant masses in a new collinear kinematical configuration compared to $pp \rightarrow hh + X$, the disagreement of full and effective theories is large (Fig. 5).

Given these shortcomings of the effective theory, we implement the full matrix element in the VBFNLO framework using FEYNARTS/FORMCALC/LOOPTOOLS. We have checked our phase space implementation for the effective theory's matrix element against MADEVENT. Some of the contributing Feynman graphs to the dominant gg -initiated subprocess are shown in Fig. 4; note that again only a subset of the contributing diagrams is sensitive to non-standard hhh couplings. Interference between these and the remaining contributions is again obvious from Fig. 8 especially at around $m_h \lesssim m_t$, which can again be explained along the lines of Sec. II B.

In comparison to $pp \rightarrow hh + X$, we find sizably larger dependence on λ of the total cross section, Fig. 8. For $p_{T,j} \geq 20$ GeV we have $\Delta\sigma/\sigma_{\text{SM}} \simeq 100\%$ for a variation $0 \leq \lambda \leq 2\lambda_{\text{SM}}$. This is due to the larger available phase space for the diHiggs system. The intermediate s channel Higgs in Fig. 4 (a), (c) is probed at smaller values compared to Fig. 1 (c), suppression is ameliorated and

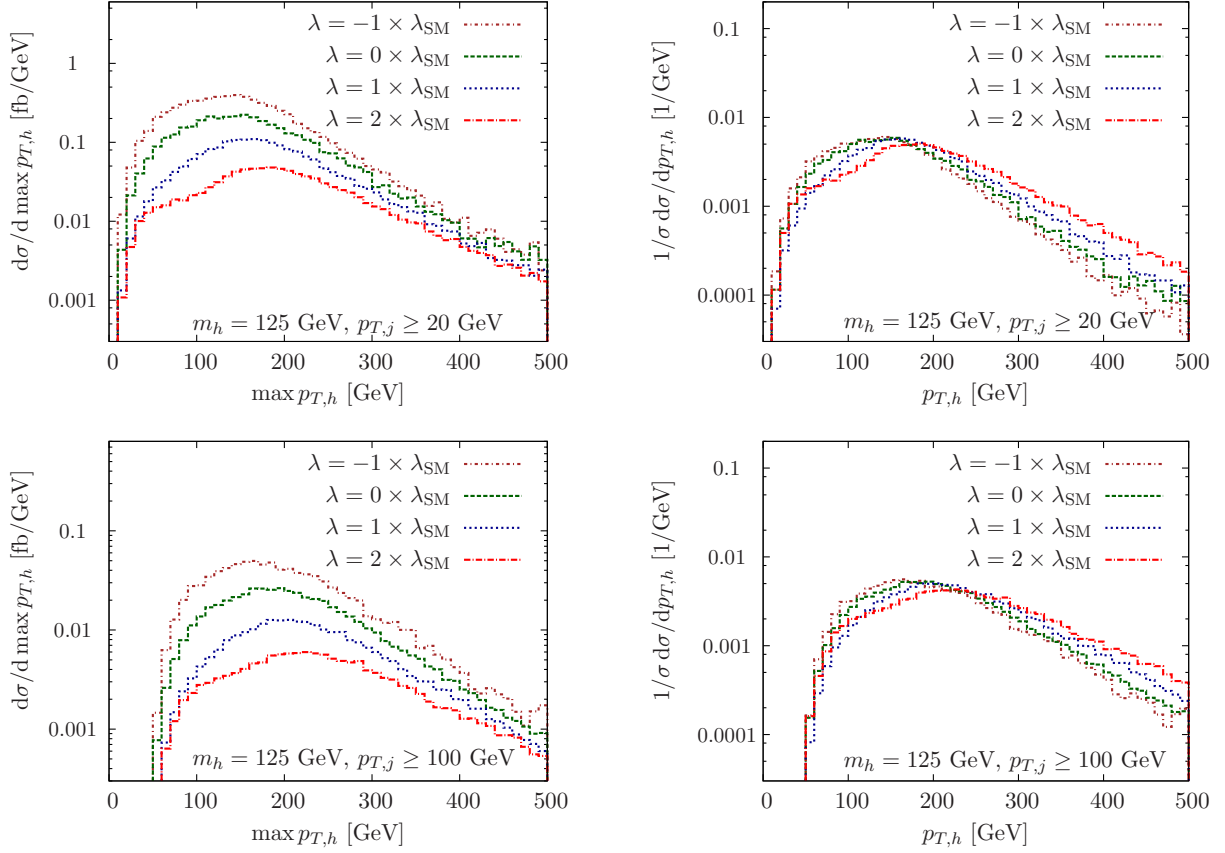


FIG. 6: Comparison of the (normalized) $\max p_{T,h}$ distributions in $pp \rightarrow hh + j + X$ for different multiples of the trilinear Higgs coupling λ ($m_t = 172.5$ GeV and $m_b = 4.5$ GeV using CTEQ61l parton densities), and $p_{T,j} \geq 20$ (100) GeV in the upper (lower) row, respectively. Factorization and renormalization scales are chosen $\mu_F = \mu_R = p_{T,j} + 2m_h$.

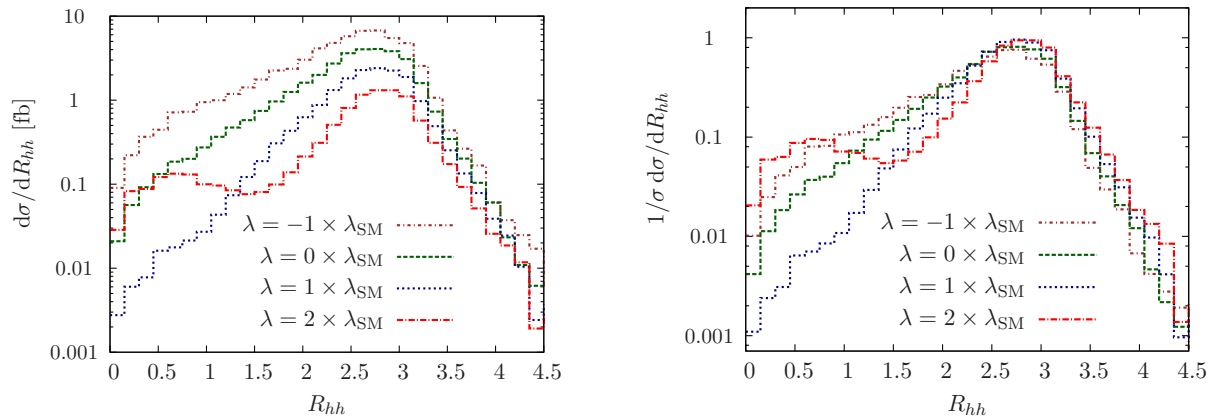


FIG. 7: Comparison of the (normalized) diHiggs lego plot separation in $pp \rightarrow hh + j + X$ for different multiples of the trilinear Higgs coupling λ ($m_t = 172.5$ GeV and $m_b = 4.5$ GeV using CTEQ61l parton densities), and $p_{T,j} \geq 100$ GeV in the upper (lower) row, respectively. Factorization and renormalization scales are chosen $\mu_F = \mu_R = p_{T,j} + 2m_h$.

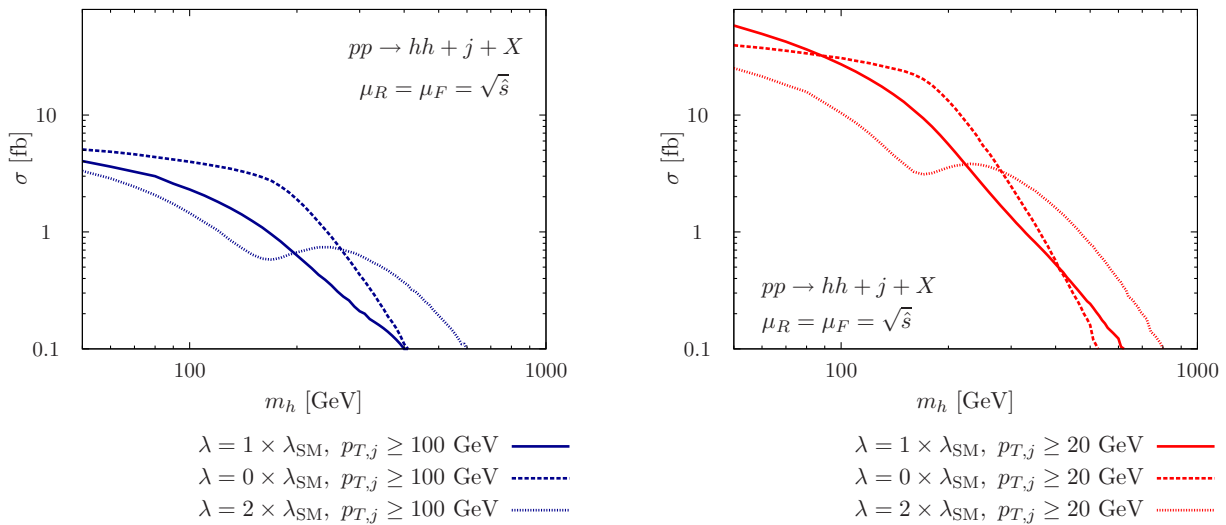


FIG. 8: Comparison of $pp \rightarrow hh + j + X$ production cross sections for three different values of the Higgs self-coupling and two values of $\min p_T^j$ (we choose identical input parameters as for Fig. 5).

(destructive) interference becomes more pronounced.

With a diHiggs system that becomes less back-to-back for increasingly harder jet emission, the characteristic dip structure encountered in the $p_{T,h}$ spectrum of $pp \rightarrow hh + X$ is washed out (Fig. 6). Characteristic imprints can still be observed in the diHiggs invariant mass or, equivalently, in the diHiggs separation in the azimuthal-angle—pseudorapidity plane, Fig. 7.

Let us summarize a few points relevant to the analysis of $pp \rightarrow b\bar{b}b\bar{b} + j + X$ production for $p_{T,j} \gtrsim 100$ GeV:

- The diHiggs+jet cross section has a comparably large dependence on the value of the trilinear couplings as compared to $pp \rightarrow hh + X$ ($\Delta\sigma/\sigma_{\text{SM}} \simeq 45\%$ when varying $\lambda \in [0, 2\lambda_{\text{SM}}]$),
- the sensitivity to non-standard values of the trilinear coupling arises from phase space configurations where the two Higgs bosons are close to each other in the central part of the detector, *i.e.* for rather small values of the invariant masses,
- as a consequence, the hadronic Higgs decay products are likely to overlap, and to fully reconstruct the busy hh decay system we need to rely on jet-substructure techniques.

Let us again comment on the impact of higher order QCD contributions. A full NLO QCD computation for $pp \rightarrow hh + j + X$ is yet missing, but most $pp \rightarrow VV + j + X$ ($V = W^\pm, Z, \gamma$) production cross sections, which have similar properties from a QCD point of view, are known to NLO QCD precision [52]. Also, the NLO QCD cross sections for $pp \rightarrow Vh + j + X$ ($V = W^\pm, Z$) have been provided in Ref. [53]. Given that the QCD sector is largely agnostic about the matrix elements' precise electroweak properties (taken apart the partonic composition of the

initial state), it is not a big surprise that all these production cross sections exhibit a rather similar phenomenology at NLO QCD. The total inclusive K factors range around $K \sim 1.3$ and result from unsuppressed parton emission. It is hence reasonable to expect the QCD corrections to $pp \rightarrow hh + j + X$ to be of similar size, and parton shower Monte Carlo programs to reasonably reproduce the dominant kinematical properties.

B. Boosted Higgs searches in association with a jet

From Fig. 6 we see that the Higgs bosons are again naturally boosted. Events of this signature possess an hadronically more active final state. The pure BDRS approach works very well if there is no other hard radiation inside the fatjet except the decay products of the Higgs boson. Here it is likely that the additional hard jet ends up in one of the fatjets challenging a good reconstruction of the Higgs. Therefore, we modify the tagger similar to the Higgs tagger in [54]: The last clustering of the jet j is undone, giving two subjets j_1, j_2 , ordered such that $m_{j_1} > m_{j_2}$. If $m_{j_1} > 0.8m_j$ we discard j_2 and keep j_1 , otherwise both j_1 and j_2 are kept. For each subjet j_i that is kept, we either add it to the list of relevant substructures (if $m_i < 30$ GeV) or further decompose it recursively. After performing this declustering procedure (we do not stop after observing a mass drop but continue to decluster the jets until we obtain a set of hard subjets inside the fat jet) we recombine the constituents of every two-subjet combination with the C/A algorithm using $R_{\text{filt}} = \min(0.3, \Delta R_{j_1, j_2}/2)$. For each combination we keep the three hardest filtered subjets and call it a Higgs candidate. The two hardest filtered subjets of the Higgs candidate with the mass closest to the true Higgs mass of 125 GeV we require to be b -tagged. We find

	$\xi = 0$	$\xi = 1$	$\xi = 2$	$\bar{b}\bar{b}\bar{b}\bar{b}j$	$\bar{b}\bar{b}\bar{b}j$ elw	$\bar{b}\bar{b}\bar{b}j$ elw2	ratio to $\xi = 1$
cross section before cuts	6.45	3.24	1.81	29400	513.36	10.0	$1.1 \cdot 10^{-4}$
trigger+fatjet cuts	1.82	1.08	0.69	10579.8	211.04	4.16	$1.0 \cdot 10^{-4}$
first kinematic Higgs rec (new tagger) + $2b$	0.30	0.20	0.13	331.84	10.82	0.54	$0.5 \cdot 10^{-3}$
sec kinematic Higgs rec + $2b$	0.09	0.059	0.039	54.1	2.46	0.066	$1.0 \cdot 10^{-3}$
invariant mass + $p_{T,j}$ cut	0.049	0.031	0.022	36.06	0.92	0.030	$0.9 \cdot 10^{-3}$

TABLE IV: Signal and background cross sections in fb for $hh + j \rightarrow \bar{b}\bar{b}\bar{b}\bar{b} + j$ for boosted kinematics. The Higgs self-coupling is scaled in multiples of the Standard Model value $\lambda = \xi \times \lambda_{\text{SM}}$, Eq. (4). None of the contributing backgrounds' normalization is known to NLO QCD precision. We therefore include a conservative correction factor of $K = 2$.

that this tagger recovers roughly 40% more of the signal events while keeping S/B constant.

1. $hh + j \rightarrow \bar{b}\bar{b}\bar{b}\bar{b} + j$

We proceed in a similar manner to the analysis outlined in Sec. III B 2, but with modifications of the Higgs tagger in order to preserve a larger signal cross section. Again we veto events with isolated leptons in $|y| < 2.5$ for $p_{T,l} > 10$ GeV and $E_{T,\text{had}} < 0.1 E_{T,l}$ within $R < 0.3$. To assure the trigger requirements we ask for at least five jets and the following staggered cuts on the transverse momentum: $p_{T,j_1} > 120$ GeV, $p_{T,j_2} > 100$ GeV, $p_{T,j_3} > 70$ GeV, $p_{T,j_4} > 40$ GeV. All jets have to fall inside the detector $|y| < 4.5$. The events which pass these trigger criteria are again analyzed in a subjet approach: We reconstruct fatjets with $p_{T,j} > 150$ GeV and $R = 1.5$. At least one fatjet has to be present which fulfills the mass-drop condition [17] with an invariant mass of $m_j > 110$ GeV. The reconstructed Higgs has to be double b -tagged and have $p_{T,h} > 150$ GeV.

The hardest of these fatjets is declustered with a tagger which is inspired by the Higgs tagger of Ref. [54]. The reconstructed Higgs has to be double b -tagged with $p_{T,h} > 150$ GeV. We subsequently remove the reconstructed Higgs' constituents from the event.

The remaining constituents are reclustered using the anti-kT algorithm with $R = 0.4$ and $p_{T,j} > 30$ GeV. The two jets which reconstruct the Higgs mass best within $m_h = 125 \pm 10$ GeV are b -tagged with 60% tagging efficiency and 2% fake rate; b -tagging is again performed in $|y| < 2.5$. Then, the two jets are again removed from the event. For the two reconstructed Higgs jets we require an invariant mass $(p_{H_1} + p_{H_2})^2 > 400^2$ GeV² and the last remaining jet needs to be hard $p_T > 100$ GeV. In total, this corresponds to a signal signature discussed in Sec. III A.

The results of this analysis flow can be found in Tab. IV. For the numbers quoted there it is clear that our cut setup serves to highly reduce the contributing backgrounds, but the QCD-induced cross sections have too large initial value. In the QCD background, while the $\bar{b}\bar{b}\bar{b}\bar{b}$ was predominantly gluon initiated, the $\bar{b}\bar{b}\bar{b}\bar{b} + j$ receives large contributions from qg initial states, leading to final states with a large invariant mass. This in turn in-

creases the amount of background in searches for boosted resonances. The QCD backgrounds can be reduced by a factor $\mathcal{O}(1000)$ while the signal rate is decreased by a factor ~ 100 . In total, this does not leave a large enough S/B to be relevant from the point of systematics, and we conclude that $pp \rightarrow hh + j \rightarrow \bar{b}\bar{b}\bar{b}\bar{b} + j$ is not a sensitive channel.

2. $hhj \rightarrow \bar{b}\bar{b}\tau^+\tau^-j$

We follow closely the steps described in Sec. II D 2 and Sec. III B 1. We require exactly two τ jets in an event in $|y_\tau| < 2.5$ and assume an identification efficiency of 80% each. The τ s have to reconstruct to an invariant mass of $m_h \pm 25$ GeV. Then we use the C/A algorithm to reconstruct fatjets with $R = 1.5$ and $p_{T,j} > 150$ GeV and require at least 1 fatjet in the event which is sufficiently isolated from the τ s. Then we apply the Higgs tagger described in Sec. and require the reconstructed Higgs jet have a mass of $m_h \pm 10$ GeV and $p_{T,H} > 150$ GeV. To suppress the large $t\bar{t}$ background we reject events where the invariant mass of the two reconstructed Higgs bosons is below 400 GeV. After removing the constituents of the reconstructed Higgs bosons from the final state we cluster the remaining final state constituents using the anti-kT algorithm $R = 0.4$ and $p_{T,j} > 30$ GeV. Finally, we require at least one jet with $p_T > 100$ GeV.

We find that these cuts can suppress the backgrounds confidently as long as the τ fake rate is sufficiently small. Due the large invariant mass of the final state, several high- p_T jets and possibly leptons from the τ decays we expect that these events can be triggered on easily. The full analysis flow can be found in Tab. V. The initial background contributions are significantly lower, as this final state does not have a dominant purely QCD-induced component. In total we end up with an estimate on $S/B \simeq 1.5$. This means that with a target luminosity of 1000 fb^{-1} , constraints can be put on λ in this channel.

IV. SUMMARY

We have studied the prospects to constrain the trilinear Higgs coupling by direct measurements at the LHC in several channels, focussing on $m_h = 125$ GeV. This is

	$\xi = 0$	$\xi = 1$	$\xi = 2$	$b\bar{b}\tau^+\tau^-j$	$b\bar{b}\tau^+\tau^-j$ [ELW]	$t\bar{t}j$	ratio to $\xi = 1$
cross section before cuts	6.45	3.24	1.81	66.0	1.67	106.7	$1.9 \cdot 10^{-2}$
2τ s	0.44	0.22	0.12	37.0	0.94	7.44	$4.8 \cdot 10^{-3}$
Higgs rec. from taus + fatjet cuts	0.29	0.16	0.10	2.00	0.150	0.947	$5.1 \cdot 10^{-2}$
kinematic Higgs rec.	0.07	0.04	0.02	0.042	0.018	0.093	0.26
$2b + hh$ invariant mass + $p_{T,j}$ cut	0.010	0.006	0.004	<0.0001	0.0022	0.0014	1.54

TABLE V: Signal and background cross sections in fb for $hh+j \rightarrow b\bar{b}\tau^+\tau^-+j$ for boosted kinematics. The Higgs self-coupling is scaled in multiples of the Standard Model value $\lambda = \xi \times \lambda_{\text{SM}}$, Eq. (4). The QCD corrections to $t\bar{t}+j$ have been discussed in Ref. [51] ($K \simeq 1.1$). For the pure electroweak production we take the results of [52] as a reference value ($K \simeq 1.3$). The corrections to mixed production are unknown and we conservatively use a total inclusive QCD correction $K = 2$.

also the mass region which is preferred by electroweak precision data, and where we currently observe excesses in data both at the LHC and the Tevatron. Depending on the particular decay channel, we find a promising signal-to-background ratio at the price of a very small event rate.

Higgs self-coupling measurements for a SM Higgs in this particular mass range are typically afflicted with large backgrounds, so that achieving maximal sensitivity requires the combination of as many channels as possible. For dedicated selection cuts we obtain signal cross sections in Higgs pair production of the order of 0.01 to 0.1 fb and measurements will therefore involve large data sets of the 14 TeV run with a good understanding of the involved experimental systematics.

Searches for unboosted kinematics of the Higgs bosons do not allow any constraint on the trilinear coupling or total cross-section to be made. However, requiring the two Higgses to be boosted and applying subjet methods to boosted $pp \rightarrow hh+X$ and $pp \rightarrow hh+j+X$ production, we find a sensitive S/B particularly for final states involving decays into τ s. A necessary condition for sensitivity in these channels is a sufficiently good τ reconstruction, but more importantly, a small fake rate. Unfortunately, while boosting the Higgses increases S/B , it leads us into a region of phase space which lacks sensitivity to the trilinear coupling.

In addition to inclusive dihiggs production we find that

dihiggs production in association with a hard jet shows an improved sensitivity to the trilinear Higgs coupling. However to exploit this scenario still requires the use of boosted techniques which require thorough evaluation on data.

Assuming the efficiency for τ -tagging and the hadronic Higgs reconstruction as outlined in this work are confirmed using data, the $b\bar{b}\tau^+\tau^-$ and $b\bar{b}\tau^+\tau^-+j$ channels can be used to constrain the Higgs self-coupling in the SM at the LHC with a data set of several hundred inverse femtobarns. The analysis strategies developed in this paper will also help to improve bounds on dihiggs production in scenarios with strong electroweak symmetry breaking and related models, which also predict enhanced dihiggs production cross sections [8, 55].

Acknowledgements

CE acknowledges funding by the Durham International Junior Research Fellowship scheme and helpful conversations with P. M. Zerwas. CE also thanks the CERN theory group, and MJD the Bonn theory group, for hospitality during the time when this work was completed. We cordially thank the members of the Institute for Particle Physics Phenomenology for their patience during the time when we were occupying the entire cluster, and especially Mike Johnson and Peter Richardson for the cluster-support.

-
- [1] F. Englert and R. Brout, Phys. Rev. Lett. **13** (1964) 321. P. W. Higgs, Phys. Lett. **12** (1964) 132 and Phys. Rev. Lett. **13** (1964) 508. G. S. Guralnik, C. R. Hagen and T. W. B. Kibble, Phys. Rev. Lett. **13** (1964) 585.
- [2] ATLAS collaboration, ATLAS-CONF-2012-019. CMS collaboration, CMS-PAS-HIG-12-008.
- [3] R. Barate *et al.*, Phys. Lett. B **565** (2003) 61.
- [4] TEVNPH (Tevatron New Phenomena and Higgs Working Group) and CDF and D0 Collaborations, arXiv:1203.3774 [hep-ex].
- [5] C. Englert, T. Plehn, M. Rauch, D. Zerwas and P. M. Zerwas, Phys. Lett. B **707** (2012) 512. D. Carmi, A. Falkowski, E. Kuflik and T. Volansky, arXiv:1202.3144 [hep-ph]. A. Azatov, R. Contino and J. Galloway, arXiv:1202.3415 [hep-ph]. J. R. Espinosa, C. Grojean, M. Muhlleitner and M. Trott, arXiv:1202.3697 [hep-ph]. P. P. Giardino, K. Kannike, M. Raidal and A. Strumia, arXiv:1203.4254 [hep-ph]. M. Klute, R. Lafaye, T. Plehn, M. Rauch and D. Zerwas, arXiv:1205.2699 [hep-ph]. J. R. Espinosa, M. Muhlleitner, C. Grojean and M. Trott, arXiv:1205.6790 [hep-ph].
- [6] T. Plehn, D. L. Rainwater and D. Zeppenfeld, Phys. Rev. Lett. **88** (2002) 051801. B. E. Cox, J. R. Forshaw and A. D. Pilkington, Phys. Lett. B **696** (2011) 87. C. Englert, M. Spannowsky and M. Takeuchi, arXiv:1203.5788 [hep-ph].
- [7] R. Lafaye, T. Plehn, M. Rauch, D. Zerwas and M. Duhrssen, JHEP **0908** (2009) 009. M. Rauch,

- arXiv:1203.6826 [hep-ph].
- [8] R. Contino, M. Ghezzi, M. Moretti, G. Panico, F. Piccinini and A. Wulzer, arXiv:1205.5444 [hep-ph].
- [9] U. Baur, T. Plehn and D. L. Rainwater, Phys. Rev. D **69**, 053004 (2004).
- [10] U. Baur, T. Plehn and D. L. Rainwater, Phys. Rev. D **67**, 033003 (2003).
- [11] U. Baur, T. Plehn and D. L. Rainwater, Phys. Rev. Lett. **89** (2002) 151801.
- [12] D. J. Miller, 2 and S. Moretti, Eur. Phys. J. C **13**, 459 (2000). J. A. Aguilar-Saavedra *et al.* [ECFA/DESY LC Physics Working Group Collaboration], hep-ph/0106315. V. Barger, T. Han, P. Langacker, B. McElrath and P. Zerwas, Phys. Rev. D **67** (2003) 115001.
- [13] T. Plehn and M. Rauch, Phys. Rev. D **72** (2005) 053008.
- [14] T. Plehn, M. Spira and P. M. Zerwas, Nucl. Phys. B **479** (1996) 46 [Erratum-ibid. B **531** (1998) 655]. See also M. Spira, HPAIR <http://people.web.psi.ch/spira/proglist.html>.
- [15] S. Dawson, S. Dittmaier and M. Spira, Phys. Rev. D **58** (1998) 115012.
- [16] E. W. N. Glover and J. J. van der Bij, Nucl. Phys. B **309** (1988) 282.
- [17] J. M. Butterworth, A. R. Davison, M. Rubin and G. P. Salam, Phys. Rev. Lett. **100** (2008) 242001. A. Abdesselam, E. B. Kuutmann, U. Bitenc, G. Brooijmans, J. Butterworth, P. Bruckman de Renstrom, D. Buarque Franzosi and R. Buckingham *et al.*, Eur. Phys. J. C **71**, 1661 (2011). A. Altheimer, S. Arora, L. Asquith, G. Brooijmans, J. Butterworth, M. Campanelli, B. Chappleau and A. E. Cholakian *et al.*, J. Phys. G **39**, 063001 (2012).
- [18] D. E. Soper and M. Spannowsky, JHEP **1008**, 029 (2010). J. -H. Kim, Phys. Rev. D **83**, 011502 (2011). J. Thaler and K. Van Tilburg, JHEP **1103**, 015 (2011). D. E. Soper and M. Spannowsky, Phys. Rev. D **84**, 074002 (2011). S. D. Ellis, A. Hornig, T. S. Roy, D. Krohn and M. D. Schwartz, Phys. Rev. Lett. **108**, 182003 (2012).
- [19] The Atlas collaboration, ATLAS-CONF-2011-073.
- [20] M. A. Shifman, A. I. Vainshtein, M. B. Voloshin and V. I. Zakharov, Sov. J. Nucl. Phys. **30** (1979) 711 [Yad. Fiz. **30** (1979) 1368].
- [21] K. Arnold, M. Bahr, G. Bozzi, F. Campanario, C. Englert, T. Figy, N. Greiner and C. Hackstein *et al.*, Comput. Phys. Commun. **180** (2009) 1661. K. Arnold, J. Bellm, G. Bozzi, M. Brieg, F. Campanario, C. Englert, B. Feigl and J. Frank *et al.*, arXiv:1107.4038 [hep-ph].
- [22] T. Hahn, Comput. Phys. Commun. **140** (2001) 418. T. Hahn and M. Perez-Victoria, Comput. Phys. Commun. **118**, 153 (1999).
- [23] E. Boos, M. Dobbs, W. Giele, I. Hinchliffe, J. Huston, V. Ilyin, J. Kanzaki and K. Kato *et al.*, hep-ph/0109068.
- [24] A. L. Read, J. Phys. G **G28** (2002) 2693-2704.
- [25] M. Glück, E. Reya and A. Vogt, Z. Phys. C53 (1992) 127.
- [26] J. Pumplin, D. R. Stump, J. Huston, H. L. Lai, P. M. Nadolsky and W. K. Tung, JHEP **0207** (2002) 012.
- [27] H. M. Georgi, S. L. Glashow, M. E. Machacek and D. V. Nanopoulos, Phys. Rev. Lett. **40** (1978) 692D. S. Dawson, Nucl. Phys. B **359** (1991) 283. A. Djouadi, M. Spira and P. M. Zerwas, Phys. Lett. B **264** (1991) 440. D. Graudenz, M. Spira and P. M. Zerwas, Phys. Rev. Lett. **70** (1993) 1372.
- [28] G. Bevilacqua, M. Czakon, A. van Hameren, C. G. Papadopoulos and M. Worek, JHEP **1102**, 083 (2011). A. Denner, S. Dittmaier, S. Kallweit and S. Pozzorini, Phys. Rev. Lett. **106** (2011) 052001.
- [29] J. Ohnemus, Phys. Rev. D **44** (1991) 1403. J. Ohnemus, Phys. Rev. D **44** (1991) 3477. J. Ohnemus, Phys. Rev. D **47** (1993) 940. J. Ohnemus, J. F. Owens, Phys. Rev. D **D43** (1991) 3626.
- [30] S. Dittmaier *et al.* [LHC Higgs Cross Section Working Group Collaboration], arXiv:1101.0593 [hep-ph].
- [31] A. Djouadi, J. Kalinowski and M. Spira, Comput. Phys. Commun. **108**, 56 (1998).
- [32] C. Hackstein and M. Spannowsky, Phys. Rev. D **82** (2010) 113012. C. Englert, C. Hackstein and M. Spannowsky, Phys. Rev. D **82** (2010) 114024.
- [33] T. Gleisberg, S. Hoeche, F. Krauss, M. Schonherr, S. Schumann, F. Siegert and J. Winter, JHEP **0902** (2009) 007.
- [34] J. Alwall, M. Herquet, F. Maltoni, O. Mattelaer and T. Stelzer, JHEP **1106** (2011) 128.
- [35] M. Bahr, S. Gieseke, M. A. Gigg, D. Grellscheid, K. Hamilton, O. Latunde-Dada, S. Platzer and P. Richardson *et al.*, Eur. Phys. J. C **58** (2008) 639.
- [36] N. Greiner, A. Guffanti, T. Reiter and J. Reuter, Phys. Rev. Lett. **107** (2011) 102002.
- [37] J. M. Campbell and R. K. Ellis, Phys. Rev. D **62**, 114012 (2000). J. M. Campbell, hep-ph/0105226.
- [38] J. M. Campbell, R. K. Ellis and C. Williams, JHEP **1107**, 018 (2011)
- [39] M. Cacciari and G. P. Salam, Phys. Lett. B **641**, 57 (2006). M. Cacciari, G. P. Salam and G. Soyez, Eur. Phys. J. C **72** (2012) 1896.
- [40] See *e.g.* The Atlas collaboration ATLAS-CONF-2012-043.
- [41] N. D. Christensen and C. Duhr, Comput. Phys. Commun. **180** (2009) 1614.
- [42] C. Degrande, C. Duhr, B. Fuks, D. Grellscheid, O. Mattelaer and T. Reiter, Comput. Phys. Commun. **183** (2012) 1201.
- [43] Y. L. Dokshitzer, G. D. Leder, S. Moretti and B. R. Webber, JHEP **9708** (1997) 001 [hep-ph/9707323].
- [44] M. Wobisch and T. Wengler, In *Hamburg 1998/1999, Monte Carlo generators for HERA physics* 270-279 [hep-ph/9907280].
- [45] M. Cacciari, G. P. Salam and G. Soyez, JHEP **0804** (2008) 063 [arXiv:0802.1189 [hep-ph]].
- [46] D. L. Rainwater, D. Zeppenfeld and K. Hagiwara, Phys. Rev. D **59** (1998) 014037.
- [47] T. Plehn, D. L. Rainwater and D. Zeppenfeld, Phys. Rev. D **61** (2000) 093005.
- [48] CMS Collaboration, arXiv:1202.4083 [hep-ex].
- [49] M. Heldmann, D. Cavalli, ATL-PHYS-PUB-2006-008, ATL-COM-PHYS-2006-010.
- [50] The Atlas collaboration, ATL-PHYS-PUB-2009-088.
- [51] K. Melnikov and M. Schulze, Nucl. Phys. B **840**, 129 (2010).
- [52] V. Del Duca, F. Maltoni, Z. Nagy and Z. Trocsanyi, JHEP **0304** (2003) 059. S. Dittmaier, S. Kallweit and P. Uwer, Phys. Rev. Lett. **100** (2008) 062003. F. Campanario, C. Englert, M. Spannowsky and D. Zeppenfeld, Europhys. Lett. **88** (2009) 11001. T. Binoth, T. Gleisberg, S. Karg, N. Kauer and G. Sanguinetti, Phys. Lett. B **683** (2010) 154. F. Campanario, C. Englert, S. Kallweit, M. Spannowsky and D. Zeppenfeld, JHEP **1007**

- (2010) 076.
- [53] S. Ji-Juan, M. Wen-Gan, Z. Ren-You and G. Lei, Phys. Rev. D **81** (2010) 114037 S. Ji-Juan, G. Lei, M. Wen-Gan, Z. Ren-You, L. Liu-Sheng and H. Liang, JHEP **1203**, 059 (2012)
- [54] T. Plehn, G. P. Salam and M. Spannowsky, Phys. Rev. Lett. **104** (2010) 111801.
- [55] R. Grober and M. Muhlleitner, JHEP **1106**, 020 (2011). J. R. Espinosa, C. Grojean and M. Muhlleitner, JHEP **1005** (2010) 065.